Structural, vibrational, electronic, and luminescence properties of the cyclotetravanadates $A_2M(VO_3)_4$ (A=Na,Ag; M=Ca,Sr)

V. G. Zubkov, L. L. Surat, A. P. Tyutyunnik, I. F. Berger, N. V. Tarakina, B. V. Slobodin, M. V. Kuznetsov, T. A. Denisova, N. A. Zhuravlev, L. A. Perelyaeva, I. V. Baklanova, I. R. Shein, and A. L. Ivanovskii
Institute of Solid State Chemistry, Ural Branch of the Russian Academy of Sciences, Ekaterinburg GSP-145, 620041, Russia

B. V. Shulgin, A. V. Ishchenko, and A. N. Tcherepanov
Ural State Technical University, Ekaterinburg K-2, Mira Street 19, 620002, Russia

G. Svensson* and B. Forslund
Divisions of Structural and Inorganic Chemistry, Stockholm University, SE-106 91 Stockholm, Sweden

M. Yu. Skripkin
Division of Chemistry, Saint-Petersburg State University, Universitetsky Prospekt 26, 198904 Saint-Petersburg, Russia
(Received 25 April 2007; revised manuscript received 24 January 2008; published 20 May 2008)

The physical properties of the family of cyclotetravanadates $A_2M(VO_3)_4$, where A=Na,Ag and M=Ca,Sr, have been studied by means of x-ray powder diffraction, neutron diffraction, electron diffraction, infrared, Raman, NMR, photoexcitation and pulse cathode beam excitation, and x-ray photoelectron spectroscopies, and band structure calculations. The differences between the structural, vibrational, luminescence, and electronic properties of the alkali metal-containing [$Na_2Ca(VO_3)_4$ and $Na_2Sr(VO_3)_4$] and the d metal-containing cyclotetravanadates [$Ag_2Ca(VO_3)_4$ and $Ag_2Sr(VO_3)_4$] are analyzed. $Na_2Ca(VO_3)_4$, $Ag_2Ca(VO_3)_4$, $Na_2Sr(VO_3)_4$, and $Ag_2Sr(VO_3)_4$ have tetragonal structures, $P4/nbm$, with a=10.438 49(6), 10.445 24(5), 10.634 49(4), and 10.625 74(6), and c=4.938 73(5), 4.968 45(5), 4.962 05(4), and 4.979 30(4) Å, respectively. The main structural feature of $A_2M(VO_3)_4$ is the tetracyclic [V_4O_{12}] units. The hybridized O $2p$–V $3d$ states of the tetracyclic [V_4O_{12}] units have a dominant influence on the electronic structure of these compounds. The compounds are semiconducting with a local density approximation band gap increasing from 1.85 eV for $Ag_2Ca(VO_3)_4$ to 3.02 eV for $Na_2Ca(VO_3)_4$. The prospects of these compounds as advanced materials for detectors of photon and corpuscular radiation as well as for color correction of light emission sources such as lamp and light emitting diode sources are discussed.

DOI: 10.1103/PhysRevB.77.174113 PACS number(s): 61.05.cp, 61.05.fm, 78.30.−j, 87.64.K−

I. INTRODUCTION

Ternary and quaternary vanadates exhibit a fascinating variety of physical properties and are therefore widely used as advanced materials such as phosphors, optical switches, chemical sensors, and catalysts and in solid-state batteries.[1–7] The origin of the functional properties of these materials is closely related to the structural and electronic peculiarities of the compounds.

Among vanadates, a large variety of crystal structures are found. The main building blocks in these structures are various extended units of vanadium-oxygen polyhedra, e.g., low-dimensional (chains, sheets) to more complex three-dimensional blocks. The preference for a certain geometric form is mainly determined by the electron configuration of the vanadium atoms.[4] Recently, we successfully prepared[5] and investigated[6,7] a group of alkali metal-strontium vanadates, namely, $A_2Sr(VO_3)_4$, where A=Na, K, Rb, and Cs. The unique structural feature of these materials is that their crystal frameworks are built of isolated so-called tetracyclic units [V_4O_{12}], which are formed by four [VO_4] tetrahedra whose vertices are linked via shared oxygen atoms. Note that this is a rather rare structural type. Related structures have been reported only for the $M_2M'(XO_3)_4$ oxides wherein the [X_4O_{12}] tetracycles are formed by the p elements (X=P or As),[8–12] although quite recently the compound $CaY_2(GeO_3)_4$, with four-membered [GeO_4] rings of tetrahedra, has been prepared.[13]

The detailed investigations of luminescence spectrum parameters of $A_2Sr(VO_3)_4$ under photoexcitation, x-ray, and pulse electron beam excitations demonstrate that these materials may be interesting materials in the development of detectors with a selective sensitivity for photon and corpuscular radiations. It was also established[6,7] that a replacement of the alkali metals, i.e., going from $Na_2Sr(VO_3)_4$ to $Cs_2Sr(VO_3)_4$, leads to a continuous change in the structure. The coordination polyhedron around the alkali metal transforms from an octahedron to a hexagonal prism and that around the strontium from a square antiprism to a square prism. These changes affect the electronic structure of the cyclotetravanadates $A_2Sr(VO_3)_4$, whose valence band (VB) spectra are mainly composed of hybridized O $2p$–V $3d$ states with very small admixtures of valence orbitals of the other components (alkali metals and Sr).

The interesting properties found for this family of compounds motivate the studies of how to further improve them. This can, in principle, be done into two ways: (i) replacing the alkali atoms by d metals, when the effect can be significant due to the addition of new d states in the valence bands, and (ii) replacing Sr by other isovalent alkaline-earth metals,

e.g., Ca, when the smaller size of the Ca can be expected to induce structural changes in the vanadate.

In the present paper, both ways mentioned above are examined. We have prepared four new $A_2M(VO_3)_4$ cyclotetravanadates, where $A=Ag,Na$; $M=Ca,Sr$. Extensive investigations of their physical properties by means of x-ray powder diffraction (XRD), neutron powder diffraction (NPD), electron diffraction (ED), IR, Raman, NMR, and x-ray photoelectron spectroscopies (XPS), and band structure calculations have been carried out. In addition, the luminescence spectra of $A_2M(VO_3)_4$ under photoexcitation and pulse cathode beam excitation have been collected and analyzed. This has made it possible to study and analyze the effect of the insertion of a *d* metal [$Ag_2Ca(VO_3)_4$ and $Ag_2Sr(VO_3)_4$] as well as the effect of substituting Sr for Ca [comparing $Na_2Sr(VO_3)_4$ and $Na_2Ca(VO_3)_4$] on the structural, vibration, electronic, and luminescence properties of these cyclotetravanadates. Note that the syntheses of the Na-Ca, Ag-Ca, and Ag-Sr vanadates have been also reported in Refs. 14 and 15.

The paper is organized as follows: In Sec. II, the experimental methods and band structure calculation procedure are described. Section III will be devoted to results obtained concerning the crystal structure, vibration, luminescence, and electronic properties of these materials. The conclusions are given in Sec. IV.

II. EXPERIMENTAL AND COMPUTATIONAL DETAILS

The compounds $A_2M(VO_3)_4$, ($A=Ag,Na$; $M=Ca,Sr$) were prepared by a solid-state route from the starting materials $AgNO_3$ (99.99%), Na_2CO_3 (99.99%), $SrCO_3$ (99.9%), $CaCO_3$ (99.9%), and V_2O_5 (99.99%) as discussed in Ref. 6. All of the XRD patterns were collected at room temperature on a STADI-P automated diffractometer (STOE, Germany) by using Cu $K\alpha_1$ radiation and a mini-PSD in the 2θ range from 2° to 100° with a step of 0.02°. Polycrystalline silicon [$\lambda=5.43075(5)$ Å] was used as external standard. The JCPDS-ICDD PDF2 database of powder standards (ICDD, USA, Release 2005) was used to identify possible impurity phases. The neutron diffraction measurements were carried out at room temperature on a D7A setup of the IVV 2M reactor (town Zarechnyi, Russia) in the 2θ range from 5° to 110° with a step of 0.05° and neutron wavelength ($\lambda=1.5322$ Å). For the analytical transmission electron microscopy studies including ED and energy-dispersive spectroscopy (EDS) x-ray microanalysis, the samples were crushed in butanol and a drop of this solution was put on a copper grid covered with a holey carbon film. The transmission electron microscope used was a JEOL 2000FX operated at 200 kV and equipped with a LINK AN10000 EDX system. The scanning electron microscopy studies were made in a JEOL JSM880 equipped with a LINK ISIS EDS system.

The crystal structure refinement was done with both the XRD and the NPD data by using the GSAS program.[16] The latter software allows simultaneous use of x-ray and neutron diffraction data in the refinements. Combining XRD and NPD data in a refinement deserves a comment since the photons are scattered by electrons and the neutrons in this case by the nuclei of the atoms. The results of separate refinements by using the XRD and the NPD data will therefore not completely coincide. However, both data have their weaknesses. For light elements, such as oxygen, the low x-ray scattering power compared to silver and vanadium can be a problem, while for neutrons, the almost zero cross section for vanadium is a limitation. We therefore decided to use one model for both data sets. The unit cell parameters were refined by using the XRD data. These values were then used with the NPD data, and the wavelength was refined.[17] The line profile was fitted by the pseudo-Voigt function, $I(2\theta)=\eta^*L(2\theta)+(1-\eta)^*G(2\theta)$ (where L and G are the Lorentzian and Gaussian, respectively), and the angular dependence of the full (line) width at half maximum (FWHM) of the reflections was described by the relation $(\mathrm{FWHM})^2=Utg^2\theta+Vtg\theta+W$. The background level was described as a combination of 15 Chebyshev polynomials.

IR and Raman-scattering measurements were used to examine how the choice of metals ($A=$Na versus Ag and $M=$Ca versus Sr) influences the torsion of the flexible tetracyclic [V_4O_{12}] units in $A_2M(VO_3)_4$. The Raman spectra were recorded on a Renishaw RM-1000 laser Raman microscope system at ambient temperature with excitation wavelength $\lambda=514.5$ nm (Ar ion laser). Both the spectral resolution and the accuracy in the Raman shift are estimated to be about 1 cm^{-1}. The IR spectra were recorded by using the KBr pellets technique in the 1200–400 cm^{-1} frequency range with a "Spectrum-One" spectrometer (PerkinElmer). The resolution was about 0.5 cm^{-1} in the investigated spectral range.

The luminescence spectra of the $A_2M(VO_3)_4$ cyclotetravanadates have been investigated under pulse cathode beam and partly photoexcitation and x-ray excitation. Photoluminescence (PL) spectra were measured with a Cary Eclipse (Varian) monochromator in the range of 400–1000 nm (1.23–3.1 eV) under excitation in the wavelength range of 220–600 nm (2.06–5.61 eV). The x-ray (40 kV, W anode) luminescence spectra were measured with an MDR-23 monochromator and a PM-106 type photomultiplier. The measurement of the pulse cathode luminescence (PCL) spectra has been carried out by means of a KLAVI-R installation with a RADAN-220 electron accelerator ($E=160-200$ keV, $\tau=2$ ns, and $j=700$ A/cm^2), an OS-13 polychromator, and a 512-element charge-coupled device camera. The parameters of the luminescent bands were extracted from the spectra by peak fitting by using a Gaussian–Lorentzian cross product distribution form,

$$A(E)=\frac{A_0}{1+f\left(\frac{E-W}{\sigma}\right)^2\exp\left[\frac{1-f}{2}\left(\frac{E-W}{\sigma}\right)^2\right]}, \quad (1)$$

where A_0 is the maximal amplitude of the band, W is center of the band, σ is the width of the band, and f defines the shape of the band (from Gaussian for $f\sim0.5$ to Lorentzian for $f=1$).

XPS measurements were carried out using a VG ESCALAB MK II electron spectrometer with Al $K\alpha_{1,2}$ x-ray excitation ($E_{h_\nu}=1486.6$ eV). The spectrometer was calibrated with the XPS of Au $4f_{7/2}$ (84.0 eV). The accuracy of

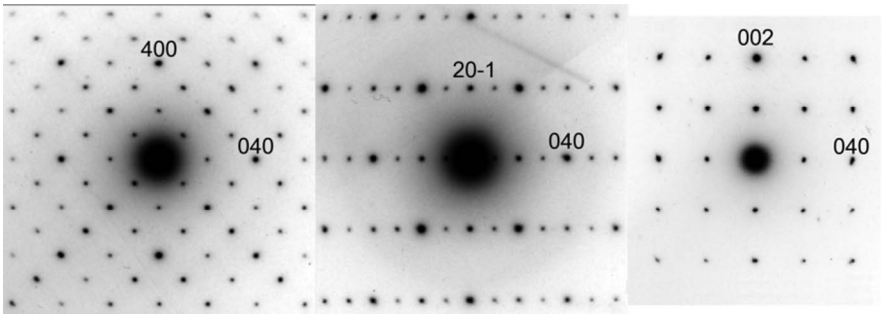

FIG. 1. A series of SAED patterns of $Na_2Ca(VO_3)_4$. The indexing corresponds to a unit cell with the space group $P4/nbm$.

the measured binding energy was 0.1 eV. The pressure in the vacuum chamber during the measurements was below 10^{-8} Pa. For all of the cyclotetravanadates, several spectra were collected: (i) a survey XPS spectrum; (ii) Na 1*s*-, Ag 3*d*-, Ca 2*p*, Sr 3*d*-, V 2*p*- and O 1*s*-core levels; and (iii) valence band spectra.

V^{51} NMR measurements were performed by using a homemade wide-line spectrometer operated at 23 MHz at room temperature. A water solution of KVO_3 was applied as a standard for the chemical shifts.[18] The shape and width of V^{51} NMR signals from $A_2M(VO_3)_4$ samples are determined by the effects of electric quadrupole coupling, magnetic dipole-dipole interactions, and anisotropy of the chemical shift. The experimental ^{51}V quadrupole coupling parameters [C_Q are quadrupole coupling constants and η_Q are parameters of the asymmetry of the electric-field gradient (EFG)] were evaluated with a line-shape generated program.

Band structure calculations for all of the cyclotetravanadates were performed by using the full-potential LAPW+lo method (FLAPW; code WIEN2K).[19] The spherical radii were 2.2 a.u. for Sr and Ca, 2.22 a.u. for Ag and Na, 1.52 a.u. for V, and 1.34 a.u. for oxygen. The plane-wave cutoff was at $R_{mt}K_{\max}=9$. The generalized gradient approximation (GGA) of Perdew *et al.*[20] was used for exchange-correlation potential. The modified tetrahedron method of Blöchl *et al.*[21] was employed for the calculation of total and site-projected density of state (DOS).

III. RESULTS AND DISCUSSION

A. Crystal structure

The ED, XRD, and NPD data indicate all of the cyclotetravanadates $A_2M(VO_3)_4$ (A=Na, Ag; M=Ca, Sr) to be isostructural with the compounds earlier studied,[6,7,14,15] where A=K, Rb, and Cs and M=Sr. As representative for the selected area electron diffraction (SAED) patterns of $A_2M(VO_3)_4$, those for $Na_2Ca(VO_3)_4$ viewed along the [001], [102], and [100] zone axes are depicted in Fig. 1. The systematic absences of reflexes ($hk0$: $h+k=2n$) along the zone axis [001] are in agreement with the space group $P4/nbm$. The presence of forbidden $0kl$ $k\neq 2$ type reflexes in the [100] and [102] zone axis patterns is due to double diffraction. In the $A_2M(VO_3)_4$ cyclotetravanadates, the A atoms occupy the 4*f* sites, M atoms the 2*b* sites, vanadium atoms the 8*k* sites, and oxygen atoms O(1) and O(2) the 8*m* and 16*n* positions, respectively. Tables I and II present the refined structural data for these compounds; Fig. 2 illustrates their crystal structure; for details, see also Refs. 6 and 7.

The main structural difference between the $A_2M(VO_3)_4$ vanadates in this study is the elongation of the AO_6 octahedron along the c axis. The $d_{A\text{-}O(1)}/d_{A\text{-}O(2)}$ ratio ranges from 1.064 for $Na_2Ca(VO_3)_4$ to 1.084 for $Ag_2Sr(VO_3)_4$ (see Table II). This type of tetragonal distortions can often be explained as a Jahn–Teller effect. This is not the case here, however, since Na^+ and Ag^+ are not Jahn–Teller active, and the distortion therefore has to be a characteristic of the structure.

For the sodium compounds, the average A-O interatomic distances in the octahedra exceed the sum of their ionic radii (2.37 Å), while for the silver compounds, it is slightly lower (2.50 Å).[22] This could be an effect of the anisotropy of the AO_6 octahedron. Generally, for Ag^+ ions in oxides, the bonding has a predominantly covalent character for low coordination numbers, CN=2,3,4, while it is more ionic for higher CN.[23] Moreover, Ag^+ ions have a typical Ag-O bond length of 2.37 Å in square-square planar configurations. It is slightly shorter than that observed in the equatorial plane of the octahedron (2.408 and 2.421 Å) in the present compound. This could be due to the higher coordination number in the octahedra. However, it may also be that the spherically symmetric $4d^{10}$ shell of Ag^+ (^1S state) is distorted in the strong tetragonal crystal field ($d_{A\text{-}O(1)}/d_{A\text{-}O(2)}>1$). The short Ag^+-O(2) bonds will then be predominantly covalent, and the longer Ag^+-O(1) mixed ionic-covalent bonding. This phenomenon should result in considerable redistributions of electron state densities of Ag 4*d*, V 3*d*, and O 2*p* in the valence bands when Na^+ is replaced by Ag^+, which then are reflected in the IR and Raman spectra.

B. Vibrational properties

We have used the IR and Raman-scattering techniques to examine how the choice of A and M metals influences the transformation of the flexible tetracyclic $[V_4O_{12}]$ units in $A_2M(VO_3)_4$.[7] These spectra are presented in Fig. 3; the experimental vibrational frequencies and assignment for $[V_4O_{12}]$ entity vibrations are summarized in Table III. The IR and Raman spectra of the studied isostructural compounds $A_2M(VO_3)_4$ are similar, as expected.

The vibrational IR spectra in the range of 1200–400 cm^{-1} arise from the internal vibrations of atoms in individual $[VO_4]$ tetrahedra in the rings as well as from the vibrations of atoms in $[V_4O_{12}]$ rings as a whole.[7] In the discussion below, mostly V-O stretching vibrational modes are under consideration. Deconvolution of experimental vibrational spectra was performed by using the GRAMS_32 package. The assignment of vibrational frequencies was per-

TABLE I. Structural and isotropic thermal parameters (Å^2) for the cyclotetravanadates $A_2M(VO_3)_4$ (A =Na, Ag; M=Ca, Sr). The standard deviations are given in parentheses.

Parameter		$A_2Ca(VO_3)_4$		$A_2Sr(VO_3)_4$	
		Na	Ag	Na	Ag
Space group		*P*4/*nbm*	*P*4/*nbm*	*P*4/*nbm*	*P*4/*nbm*
Z		2	2	2	2
$a=b$ (Å)		10.43849(6)	10.44524(5)	10.63449(4)	10.62574(6)
c (Å)		4.93873(5)	4.96845(5)	4.96205(4)	4.97930(4)
V (Å^3)		537.93	541.69	561.17	561.95
A	x/a	0	0	0	0
	y/b	0	0	0	0
	z/c	1/2	1/2	1/2	1/2
	$U\times 100$	2.21(2)	2.79(4)	1.61(2)	3.13(4)
M	x/a	1/4	1/4	1/4	1/4
	y/b	1/4	1/4	1/4	1/4
	z/c	1/2	1/2	1/2	1/2
	$U\times 100$	1.27(2)	1.72(2)	1.60(2)	1.90(2)
V	x/a	0.5276(1)	0.5274(1)	0.5353(2)	0.5328(1)
	y/b	1/4	1/4	1/4	1/4
	z/c	0	0	0	0
	$U\times 100$	2.04(1)	2.18(1)	1.52(2)	2.44(1)
O(1)	x/a	0.6278(1)	0.6280(2)	0.6305(2)	0.6313(1)
	y/b	0.3722(1)	0.3720(2)	0.3695(2)	0.3688(1)
	z/c	0.1486(3)	0.1446(4)	0.1553(4)	0.1524(3)
	$U\times 100$	1.19(3)	1.52(3)	1.29(3)	1.59(3)
O(2)	x/a	0.1858(1)	0.1859(1)	0.1839(1)	0.1834(1)
	y/b	0.0598(1)	0.0604(2)	0.0529(1)	0.0534(1)
	z/c	0.2399(2)	0.2422(4)	0.2352(3)	0.2350(3)
	$U\times 100$	1.27(3)	1.61(3)	1.13(3)	1.65(3)
wRp	*X* [a]	2.68	3.12	3.16	2.94
	N [a]	1.83	3.59	4.30	2.56
Rp	*X* [a]	2.10	2.40	2.23	2.25
	N [a]	1.43	2.83	3.18	2.04
$R(F^2)$	*X* [a]	3.53	3.87	6.60	3.14
	N [a]	4.98	5.33	4.73	4.85

[a]*X* and *N* mean x ray and neutron, respectively.

formed in the C_i symmetry point group and based on the exception rule (all A_g vibrations are only Raman active and all A_u species are only IR active). Because of the distortion of the idealized symmetry by the outer-sphere cations and site-symmetry conditions, this rule may not be absolutely valid in these systems; rather, different intensities of the bands in Raman and IR spectra could be the key to distinguish between the symmetry species. For stretching vibrations, not only the vibrational regions but also the exact species corresponding to different symmetry coordinates were determined, whereas for the bendings, only the spectral regions are shown. The reason is that in low frequency region, Ag-O stretchings could appear; and also the strong vibrational coupling between bending modes, especially between ring deformations and VO_2 scissoring modes, demands a far more detailed treatment.

Nine spectral regions could be easily distinguished in the experimental spectra. The highest one at 890–931 cm^{-1} corresponds to VO_2 (terminal) in-phase vibrations. The next at 723–769 cm^{-1} arises from the out-of-phase stretching modes of the same entities. The bands in the region from 500 to 587 cm^{-1} originate from ring (VO-bridging) stretching modes. The Raman bands at lower wave numbers were attributed to VO_2 scissoring (361–372 cm^{-1}), twisting (328–348 cm^{-1}), wagging (240–268 cm^{-1}), and rocking (232–238 cm^{-1}) modes. The weak Raman bands at 220 cm^{-1} [$Ag_2Ca(VO_3)_4$, $Ag_2Sr(VO_3)_4$], which are not observed in the spectra of $Na_2Ca(VO_3)_4$ and $Na_2Sr(VO_3)_4$, were tentatively assigned as symmetric Ag-O stretchings. The bands at lower frequencies originate from ring deformations and torsional modes and were not assigned.

TABLE II. The shortest interatomic distances (d) and the bond angles (w) for the cyclotetravanadates $A_2M(VO_3)_4$ (A=Na, Ag; M=Ca, Sr).

			d (Å)	
Bond	$Na_2Ca(VO_3)_4$	$Ag_2Ca(VO_3)_4$	$Na_2Sr(VO_3)_4$	$Ag_2Sr(VO_3)_4$
A-O(1)	2×2.563(2)	2×2.586(2)	2×2.603(2)	2×2.624(2)
A-O(2)	4×2.408(1)	4×2.408(2)	4×2.423(1)	4×2.421(1)
⟨A-O⟩	**2.459**	**2.467**	**2.483**	**2.488**
$d_{A\text{-}O(1)}/d_{A\text{-}O(2)}$	1.064	1.074	1.074	1.084
M-O(2)	8×2.458(1)	8×2.452(2)	8×2.572(2)	8×2.570(1)
V-O(1)	2×1.805(1)	2×1.800(1)	2×1.801(1)	2×1.806(1)
V-O(2)	2×1.638(1)	2×1.655(2)	2×1.652(2)	2×1.645(1)
⟨V-O⟩	**1.721**	**1.727**	**1.726**	**1.725**
Angle		ω (deg)		
O(1)-V-O(1)	109.2(1)	108.7(2)	111.3(2)	109.2(1)
O(1)-V-O(2)	2×109.1(1)	2×109.0(1)	2×108.4(1)	2×108.7(1)
O(1)-V-O(2)	2×108.5(1)	2×108.7(1)	2×108.8(1)	2×108.9(1)
O(2)-V-O(2)	112.4(1)	112.7(1)	111.2(2)	112.4(1)
⟨O-V-O⟩	**109.5**	**109.5**	**109.5**	**109.5**
V-O(1)-V	130.8(1)	131.8(1)	127.8(1)	129.2(1)

The strongest Raman features in every region were attributed to the totally symmetric species. These modes were observed at 928–931 cm^{-1} for terminal VO bonds and at 505–514 cm^{-1} for the ring (breathing mode). As to other modes, in-phase or out-of-phase notation was used to describe the vibrations: the first part describes the movement around the same V atom; the second in the neighboring tetrahedra.

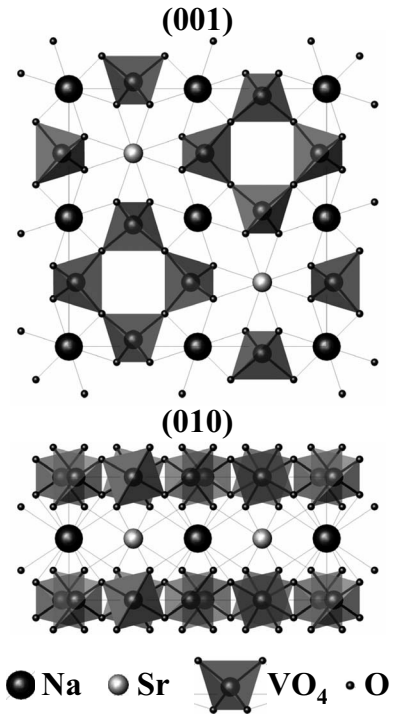

FIG. 2. Crystal structure of $A_2M(VO_3)_4$ cyclotetravanadates, where A=Na, Ag and M=Ca, Sr (space group $P4/nbm$). As an example, the projections onto the (001) and (010) planes of the crystal structure of $Na_2Sr(VO_3)_4$ are depicted.

The experimental frequencies and structural data were utilized for the calculation of stretching force constants. Wilson's GF matrix method was used. The personal-computer-based program package was developed by Mink and Mink.[24] The data are presented in Table IV. Complete cyclic V_4O_{12} entity was under consideration to avoid the problem of underestimation of the interaction between different modes in cyclic molecule.

As one can expect from common knowledge, bridging bonds should have lower bond order compared to the terminal ones. The trend in force constants agrees fairly well with this suggestion. Moreover, the force constants are more sensitive to the nature of the cations compare to the bond lengths: the last ones also reflect the packing effect, whereas the force constants do not. For example, V-O (bridging) bond length decreases from $Na_2Sr(VO_3)_4$ to $Na_2Ca(VO_3)_4$ and the force constants also decrease, which is in a good agreement with the increase in the polarization effect of the cation. The comparison of the data obtained for the compounds under study enables to reveal the effects of both monovalent and divalent cations on the bonding in the cyclic V_4O_{12} entity. As one can expect, the formation of covalent M-O bonds by the silver atom should result in some weakening of V-O bond. That is rather well pronounced in the force constants: the replacement of sodium by silver leads to the decrease in stretching force constants. This effect is more pronounced for the terminal bonds (approximately 13.5% decrease) compared to the bridged ones (9%). As to the divalent cation, the replacement of strontium by calcium also results in decrease in stretching force constants, especially in case of silver compounds. It is interesting to note that ring bonds are more sensitive to the nature of divalent cation probably because of the different conformations of the ring.

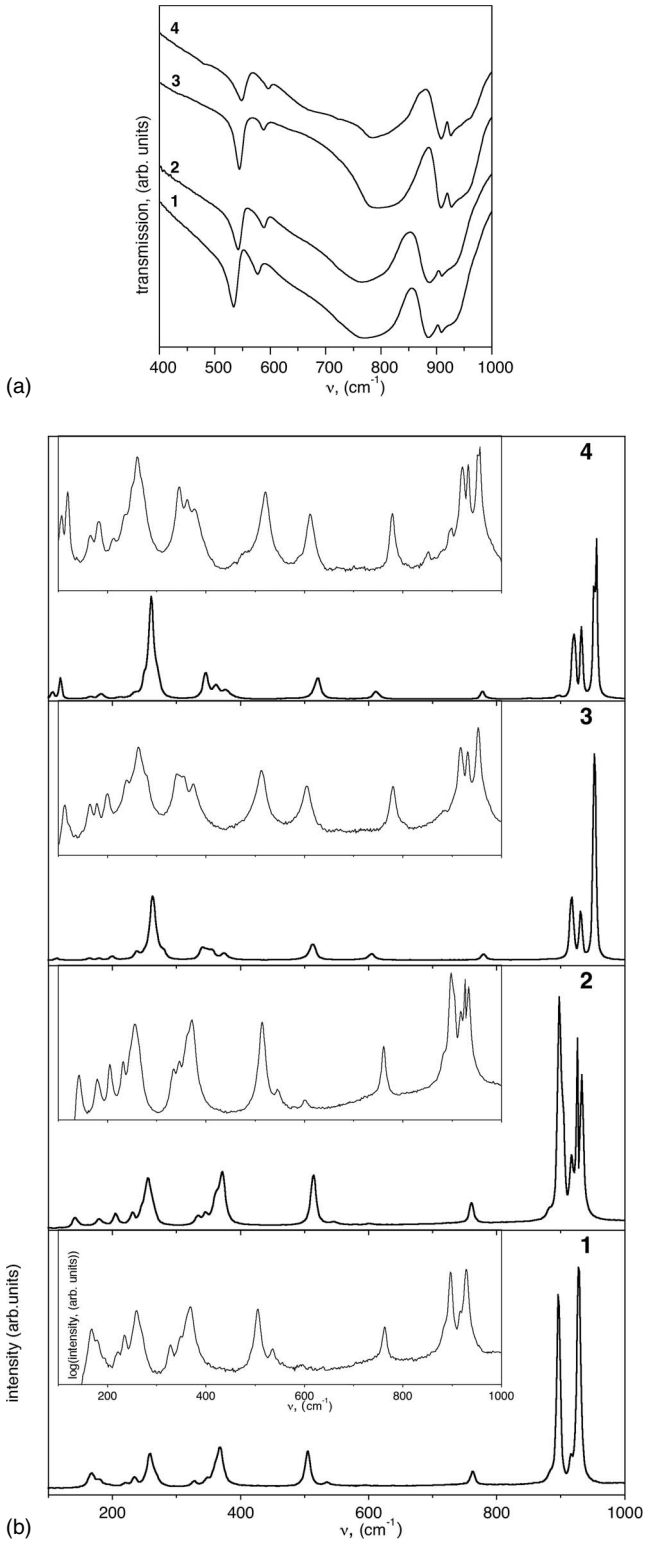

FIG. 3. (a) Infrared and (b) Raman spectra of (1) $Ag_2Ca(VO_3)_4$, (2) $Ag_2Sr(VO_3)_4$, (3) $Na_2Ca(VO_3)_4$, and (4) $Na_2Sr(VO_3)_4$.

C. Luminescence properties

The intrinsic visible luminescence spectra of investigated vanadates are presented in Figs. 4(a)–4(g) and one of excitation spectrum in Fig. 4(h). In Figs. 4(a)–4(e), the results of spectra decomposition on bands [according to expression (1)] are presented as well. At least four centers of intrinsic luminescence were found yielding four bands in the decomposition spectra: band 1 with a maximum at 515 nm (2.407 eV); band 2 with a maximum at 564–569 nm (2.198–2.179 eV); band 3 with a maximum at 629–655 nm (1.971–1.893 eV), and band 4 with a maximum at 735 nm (1.687 eV). The parameters of these bands (positions, FWHMs, amplitudes, and shapes) for all of the samples are given in Table V.

The positions of bands 2 (564–569 nm) and 3 (629–655 nm) vary between the compounds studied. A peculiarity of band 1 (515 nm) is its low intensity for Ag-containing vanadates. Figures 4(b) and 4(d) are independent of the type of excitation. It should also be noted that the replacement of Na for Ag leads to a significant redshift of the luminescence spectra. This can be connected with the absorption of 515 nm light by Ag ions or Ag clusters probably due to a strong change in electronegativity when replacing Na (0.97) for Ag (1.42). This influences the electronic excitations and the following nonradiative relaxation. For the Na-containing vanadates, band 1 has a high intensity (especially for x-ray excitation) and does not shift in energy [Figs. 4(a), 4(c), and 4(e)]. The position of band 4 (735 nm) for the PCL spectra is the same for all of the investigated compounds, but its intensity is very weak for x-ray and photoexcitation. The FWHM of the bands is quite large from 67 to 154 nm and their shapes close to Gaussian ($f \sim 0.5$). Outside of these decomposition spectra, a quite intensive narrow band of 698 nm has been found in the PL spectra under excitation with $\lambda_{exc} = 520-600$ nm. This band have also been found under $\lambda_{exc} = 240-260$ nm excitation but with a very weak intensity [Fig. 4(f)]. A scheme of possible radiative transitions for the investigated vanadates is presented in Fig. 5. The excitation levels for the centers of intrinsic luminescence are pointed out. There are two main levels of excitations at 4.9–5.1 and 6.2–8.2 eV for Na vanadate and an additional level of excitation at 1.78 eV for Ag vanadates. The high-energy band of excitation correlates with the parameters of the valence band (see below the XPS spectra in energy region of the Fermi level).

There are not enough data to explain the structure of luminescence centers and the mechanisms of luminescence. However, it is possible to note that the positions of luminescence bands for investigated vanadates are typical for the known luminescence bands of simple and complicate metavanadate, pyrovanadate, and orthovanadate (see Refs. 3–6). The nature of intrinsic luminescence centers in $A_2M(VO_3)_4$ can be connected with the relaxation (decay) of electronic excitation (including free- and self-trapped excitons) on some lattice defects in the vicinity of (V_4O_{12}) units (as on defects in YVO_4:Ho or as on F and F^+ color centers in tungstates; see Refs. 25–28), on hole O^- centers, oxygen $O_{\square}$ vacancy centers (of structures or thermal types), or on some another aggregate defects.

For all of the investigated compounds, the color coordinates (X,Y) have been determined: (0.40, 0.45) for $Na_2Ca(VO_3)_4$; (0.44, 0.49) for $Na_2Sr(VO_3)_4$; (0.55, 0.44) for $Ag_2Ca(VO_3)_4$; and (0.57, 0.43) for $Ag_2Sr(VO_3)_4$. It would be important for the problem connected to the choosing of materials for luminescence lamps and light emitting (LED) sources.

TABLE III. Experimental vibrational frequencies (cm^{-1}) for the compounds $A_2M(VO_3)_4$ and assignment for V_4O_{12} entity vibrations in the C_i point symmetry group.

$Ag_2Ca(VO_3)_4$		$Ag_2Sr(VO_3)_4$		$Na_2Ca(VO_3)_4$		$Na_2Sr(VO_3)_4$		
Raman	IR	Raman	IR	Raman	IR	Raman	IR	Assignment
928 vs	930	931 vs	929	953 vs		953 vs	960	ν_s(VO term)$_{ip/ip}(A_g)$—totally symmetric
915 w	912	917 w	916	934 s	927	932 s	926	ν_a(VO term)$_{ip/oop}(A_u)$
897 m	895	904 m	905	920 s		918 s		ν_a(VO term)$_{ip/oop}(A_g)$
890 w	887	898 sh	892		908		908	ν_a(VO term)$_{ip/ip}(A_u)$
						894vw		
						853vw		
	769		765		795		778	ν_a(VO term)$_{oop/ip}(A_u)$
763 m		769 m		781 w		785 w		ν_a(VO term)$_{oop/oop}(A_g)$
751 w		761 s		781 w		785 w		ν_a(VO term)$_{oop/ip}(A_g)$
728 w	723		765		795		778	ν_a(VO term)$_{oop/oop}(A_u)$
	577		587		588		596	ν_a(VO br)$_{oop/ip}(A_u)$
	568		587		588		596	ν_a(VO br)$_{ip/oop}(A_u)$
	535		542		544		548	ν_a(VO br)$_{oop/oop}(A_u)$
	526		542		544		548	ν_a(VO br)$_{ip/ip}(A_u)$
534 m		546 m		605 w		609 w		ν_a(VO br)$_{oop/ip}(A_g)$
508 m		546 m		605 w		609 w		ν_a(VO br)$_{oop/oop}(A_g)$
505 s		514 s		513 s		519 m		ν_s(VO br)$_{ip/ip}(A_g)$—totally symmetric, breathing mode
501 w		514 s		513 s		519 m		ν_a(VO br)$_{ip/oop}(A_g)$
						458 vw	482 sh	
369 s		372 s		375 w		377 w		VO_2 scissoring
361 m		362 m		356 w		361 w		
348 m		345 m		340 m		344 m		VO_2 twisting
328 m		334 m						
268 m		256 s		262 w		267 sh		VO_2 wagging
259 s		240 m				259 s		
235 m		233 w		238 w		232 w		VO_2 rocking
220 w		220 w						Ag-O stretching
		205 w		200 w		206 w		Ring deformations and torsional modes
194 w						194 w		
180 w		180 m		179 w		181 w		
171 m								
167 m				164 m		164 w		
		151 w						
		142 m						

D. Electronic properties

As an initial step of the XPS measurements, it was confirmed that the surface compositions of these compounds are very close to the formal stoichiometric ones $[A_2M(VO_3)_4]$ of the materials. This allows us to use the observed XPS spectra to discuss the electronic structure features such as the core levels and valence bands of the bulk materials, $A_2M(VO_3)_4$. This is also indicated by the Ag 3*d*, Na 1*s*, Ca 2*p*, and Sr 3*d*

TABLE IV. Refined stretching force constants (in N cm^{-1}).

Coordinate	$Ag_2Ca(VO_3)_4$	$Ag_2Sr(VO_3)_4$	$Na_2Ca(VO_3)_4$	$Na_2Sr(VO_3)_4$
V-O terminal	4.854	4.942	5.551	5.581
V-O bridging	2.378	2.512	2.646	2.713

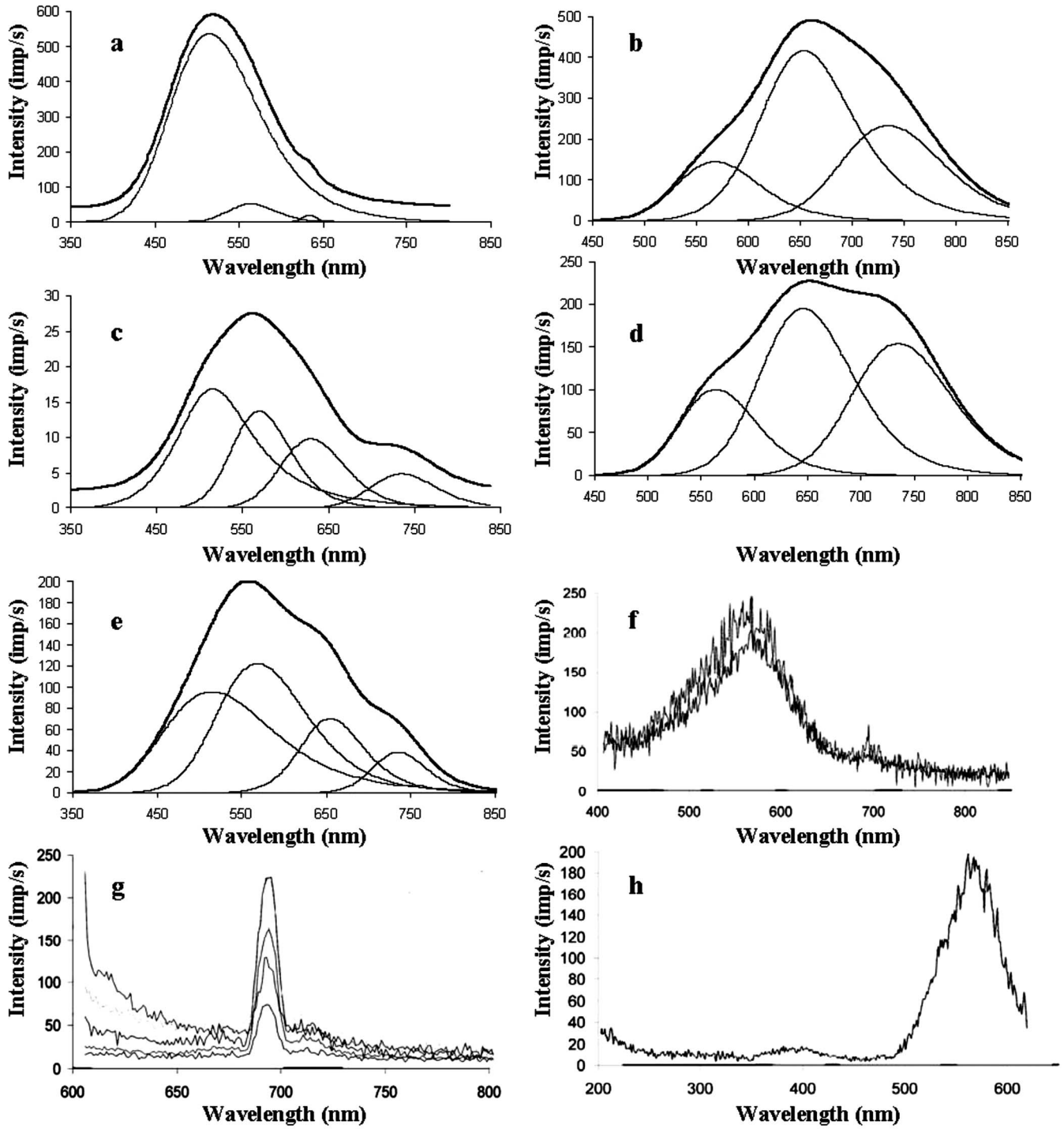

FIG. 4. Optical spectra of cyclotetravanadates: (a) x-ray luminescence spectrum of $Na_2Sr(VO_3)_4$, (b) PCL spectrum of $Ag_2Sr(VO_3)_4$, (c) PCL spectrum of $Na_2Sr(VO_3)_4$, (d) PCL spectrum of $Ag_2Ca(VO_3)_4$, (e) PCL spectrum of $Na_2Ca(VO_3)_4$, (f) PL spectrum of $Ag_2Ca(VO_3)_4$ under $\lambda=240$ nm excitation, (g) PL spectrum of $Ag_2Ca(VO_3)_4$ under $\lambda=520-560$ nm excitation, and (h) excitation spectrum of $Ag_2Ca(VO_3)_4$ for emission band $\lambda=695$ nm.

XPS spectra shown in Fig. 6. The binding energies for these core levels are presented in Table VI and allow us to conclude that Ag and Na are monovalent, whereas Ca and Sr are divalent; i.e., they have the expected formal valence states for these metals in vanadates.

The XPS spectra of the VBs from the Fermi level, $E_F=0$ up to −35 eV, for all of the $A_2M(VO_3)_4$ compounds are shown in Fig. 7. In the low-energy part of the VB for $Na_2Ca(VO_3)_4$ and $Na_2Sr(VO_3)_4$ are quasicore Na $2p$ states (around −32 eV below E_F), whereas the valence states of the other elements are located in sequence: Ca $3p$(−26.5 eV) $<$ O $2s$(−24 eV) $<$ Sr $4p$(−21 eV). The top of the valence bands (around 4–10 eV below the Fermi level) primarily comprises hybridized O $2p$–V $3d$ states. For $Ag_2Ca(VO_3)_4$

TABLE V. Parameters (centers W, FWHM, amplitude A_0, and shape f) of luminescence bands for the $A_2M(VO_3)_4$ cyclotetravanadates (A=Na, Ag; M=Sr, Ca).

Band	Parameters	$Na_2Sr(VO_3)_4$ X-ray	$Na_2Sr(VO_3)_4$ PCL	$Na_2Ca(VO_3)_4$ PCL	$Ag_2Sr(VO_3)_4$ PCL	$Ag_2Ca(VO_3)_4$ PCL
1	W (nm)	515	515	515		
	FWHM (nm)	123	69	154		
	A_0 (a.u.)	1	1	0.782		
	f	0.5	0.74	0.5		
2	W (nm)	564	569	569	568	564
	FWHM (nm)	67	81	125	94	85
	A_0 (a.u.)	0.095	0.81	1	0.346	0.514
	f	0.5	0.5	0.5	0.5	0.5
3	W (nm)	634	629	655	654	646
	FWHM (nm0	19	88	89	107	102
	A_0 (a.u.)	0.037	0.577	0.575	1	1
	f	0.5	0.5	0.6	0.6	0.5
4	W (nm)		735	735	735	735
	FWHM (nm)		91	75	116	110
	A_0 (a.u.)		0.286	0.31	0.559	0.791
	f		0.5	0.5	0.5	0.5

and $Ag_2Sr(VO_3)_4$, this region is admixed with the Ag 4d states, which suggests a non-negligible covalent contribution to the Ag-O bonds. It may also be seen in the XPS spectra that the valence bands are separated from E_F by a gap of 3–5 eV, i.e., these compounds are semiconductors. This gap is slightly smaller for the Ca-containing compounds due to a shift of the VB to lower energies for the Sr-containing ones.

These results should be compared to band structure calculations. The total densities of states (TDOSs) and site-projected, l-decomposed partial densities of states for the four cyclotetravanadates $A_2M(VO_3)_4$ are shown in Fig. 8, and their band structure parameters according to our FLAPW-GGA calculations are presented in Table VII. The main features of the valence TDOS of the $A_2M(VO_3)_4$ compounds are similar and consist of three main bands: A, B, and C (see Fig. 8). For example, for $Na_2Sr(VO_3)_4$, band A is lowest in energy and is composed of the quasicore O 2s orbitals with a small admixture of the Na 2p states. Band A contains two divided subbands formed by O 2s orbitals from the two structurally nonequivalent oxygen atoms, O(1) and O(2). The subbands with greater and smaller binding energies corresponds to O(1) and O(2) atoms forming "short" {d[O(2)-V]=1.652 Å} and "long" {d[O(1)-V]=1.801 Å} bonds in $Na_2Sr(VO_3)_4$. The following band B is exclusively formed from Sr 4p states and is separated from the near-Fermi band (C) by a wide gap of about 8.8 eV. This widest occupied band C has a combined type of O 2p states hybrid-

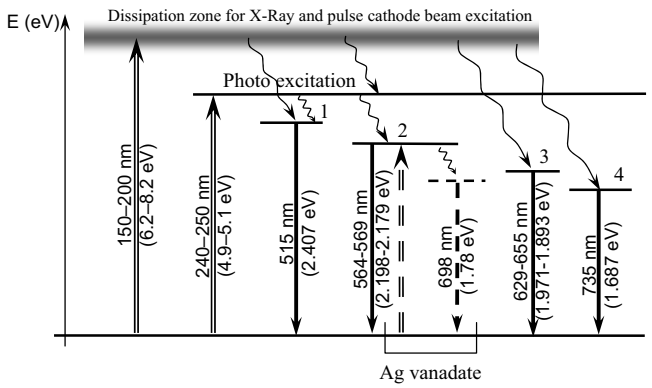

FIG. 5. Scheme of radiative relaxation of electronic excitation for cyclotetravanadates for $Na_2M(VO_3)_4$ (solid line) and $Ag_2M(VO_3)_4$ (dotted line).

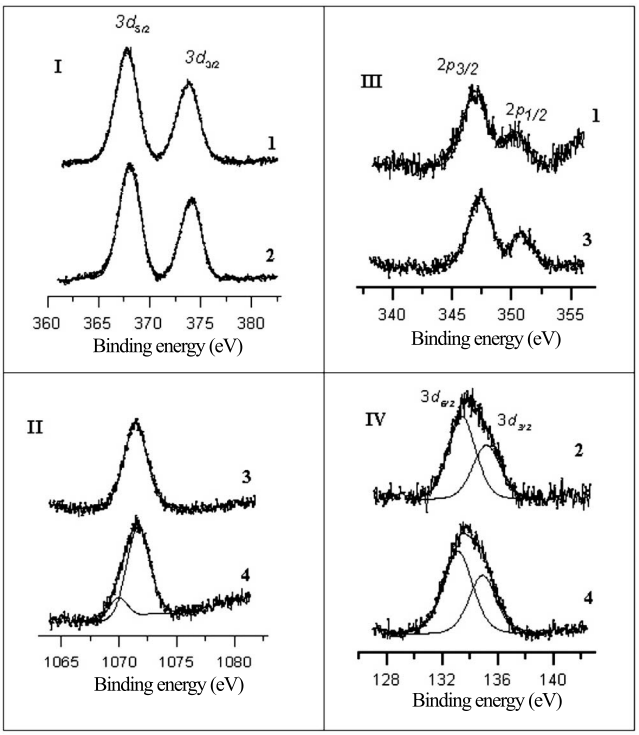

FIG. 6. XPS spectra for (i) Ag 3d-, (ii) Na 1s-, (iii) Ca 2p-, and (iv) Sr 3d-core levels in cyclotetravanadates: (1) $Ag_2Ca(VO_3)_4$, (2) $Ag_2Sr(VO_3)_4$, (3) $Na_2Ca(VO_3)_4$, and (4) $Na_2Sr(VO_3)_4$.

TABLE VI. Binding energies (in eV) for V $2p_{3/2}$, O 1*s*, Ag $3d_{5/2}$, Na 1*s*, Ca $2p_{3/2}$, and Sr $3d_{5/2}$ levels as obtained by XPS measurements for the cyclotetravanadates $Ag_2Ca(VO_3)_4$, $Ag_2Sr(VO_3)_4$, $Na_2Ca(VO_3)_4$, and $Na_2Sr(VO_3)_4$.

Vanadate	V $2p_{3/2}$	O 1*s*	Ag $3d_{5/2}$	Na 1*s*	Ca $2p_{3/2}$	Sr $3d_{5/2}$
$Ag_2Ca(VO_3)_4$	517.2	530.33	367.84		346.79	
$Ag_2Sr(VO_3)_4$	517.2	530.52	368.01			133.20
$Na_2Ca(VO_3)_4$	517.2	530.39		1071.45	347.31	
$Na_2Sr(VO_3)_4$	517.2	530.46		1071.65		133.12

ized with V 3*d* states, which are responsible for the covalent bonding in the $[VO_4]$ tetrahedra inside the tetracyclic units $[V_4O_{12}]$. Here, also two types of O 2*p* states reflecting the anisotropy of vanadium-oxygen bonds are visible. The lowest part of subband C' predominantly contains O(1)2*p* states, while the near-Fermi band (C'') comprises of the O(2)2*p* states. As a result, the top of the valence bands in the Na-containing vanadates mainly consists of 2*p* states of O(2) atoms. Note also that the contributions from the valence Sr 5*s* and Na 3*s* states in the occupied bands are negligible; i.e., in $A_2M(VO_3)_4$, these atoms are in the form of cations Sr^{2+} and Na^+. Thus, the chemical bonding in the vanadates is of mixed ionic-covalent character, i.e., predominantly ionic interactions between *A* and *M* atoms and oxygen and covalent V-O interactions in the tetracyclic $[V_4O_{12}]$ units. Alongside thus covalent V-O bonding, there is an additional ionic part in the tetracycles, which is caused by a charge transfer in the direction V→O (see also Ref. 4). The bottom of the unoccupied band (*D*, see Fig. 8) is primarily derived from antibonding V 3*d* states with an admixture of O 2*p* and Na 3*p* states. Our calculations show that $Na_2Sr(VO_3)_4$ is a semiconductor with a local density approximation (LDA) band gap (BG) of about 2.9 eV.

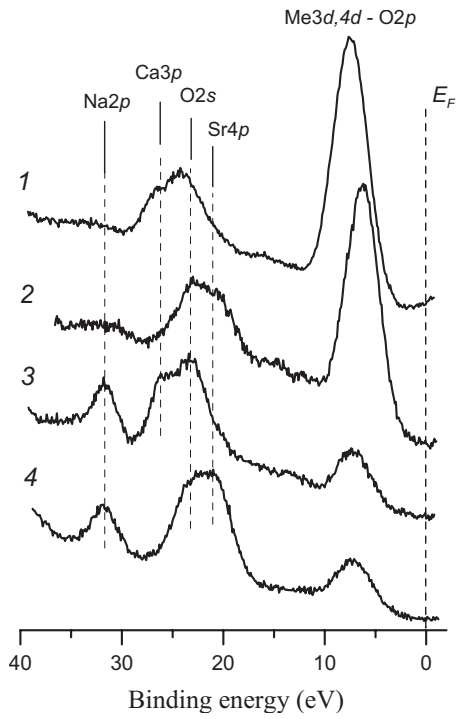

FIG. 7. XPS spectra for the valence region of (1) $Ag_2Ca(VO_3)_4$, (2) $Ag_2Sr(VO_3)_4$, (3) $Na_2Ca(VO_3)_4$, and (4) $Na_2Sr(VO_3)_4$.

Substitution of Sr^{2+} for the isovalent Ca^{2+} in the Na-containing vanadate leads to the inversion of the positions of the localized O 2*s* and alkaline-earth metal *p* bands, whereas the width of the hybrid O 2*p*–V 3*d* band and the value of the BG insignificantly change (no more than 0.1 eV; Table VII). A much more dramatic change in the $A_2M(VO_3)_4$ spectra is caused by the replacement of the alkali metal (Na) by silver in the $[AO_6]$ octahedra, as demonstrated by the DOS pictures for $Na_2Sr(VO_3)_4$ and $Ag_2Sr(VO_3)_4$ (Fig. 8). When going from $Na_2Sr(VO_3)_4$ to $Ag_2Sr(VO_3)_4$, a significant enhancement of the width for hybrid band *C* (at about 1 eV) takes place due to the admixture of occupied Ag 4*d* bands in the near-Fermi region. This effect is accompanied by a narrowing of the BG from 2.9 eV for $Na_2Sr(VO_3)_4$ to 2.1 eV for $Ag_2Sr(VO_3)_4$. In the DOS shown in Fig. 8, it can also be seen that the splitting of the Ag 3*d* orbitals is due to the above-mentioned tetragonal distortions (bond length anisotropy) of the octahedra $[AgO_6]$. The top of the valence band for $Ag_2Sr(VO_3)_4$ is of predominantly of Ag $3d_{xz,yz}$ type.

From the data presented in Table VII, it can be concluded that the replacement of *A* cations (Na↔Ag) leads to much more basic changes in the electronic properties for vanadates (due to formation of the new covalent Ag-O bonds) than replacements in the alkaline-earth metal sublattice (Sr↔Ca), where the ionic nature of bonding is retained. Furthermore, the results of FLAPW-GGA calculations concerning the main peculiarities for $A_2M(VO_3)_4$ valence spectra correlate well with those obtained from XPS measurements (Fig. 7).

It is well known that band structure methods that use the LDA lead to a typical underestimation of the band gap for insulating oxides of about 30%–60%.[29–32] According to our FLAPW-GGA data, the band gap values for vanadates are between 3.02 [for $Na_2Ca(VO_3)_4$] and 1.85 eV [for $Ag_2Ca(VO_3)_4$]. A standard empirical correction[33] means fitting the LDA gap to an experimental value. In our case, by using a suggested[34] multiplicative correction factor (1.6), from our calculations we can estimate the values of "experimental" BGs for $A_2M(VO_3)_4$, which are in interval from 4.8 to 3.0 eV, i.e., close to XPS measurements.

Finally, there are some peculiarities of electron distribution in these $A_2M(VO_3)_4$ cyclotetravanadates, as obtained from the NMR measurements and FLAPW-GGA calculations. The line shape of NMR ^{51}V spectra for a central transition ($m_I=+1/2$ $m_I=-1/2$) indicates[35] that the signals are generated by a first-order quadrupole interaction (Fig. 9). The experimentally derived and calculated ^{51}V quadrupole

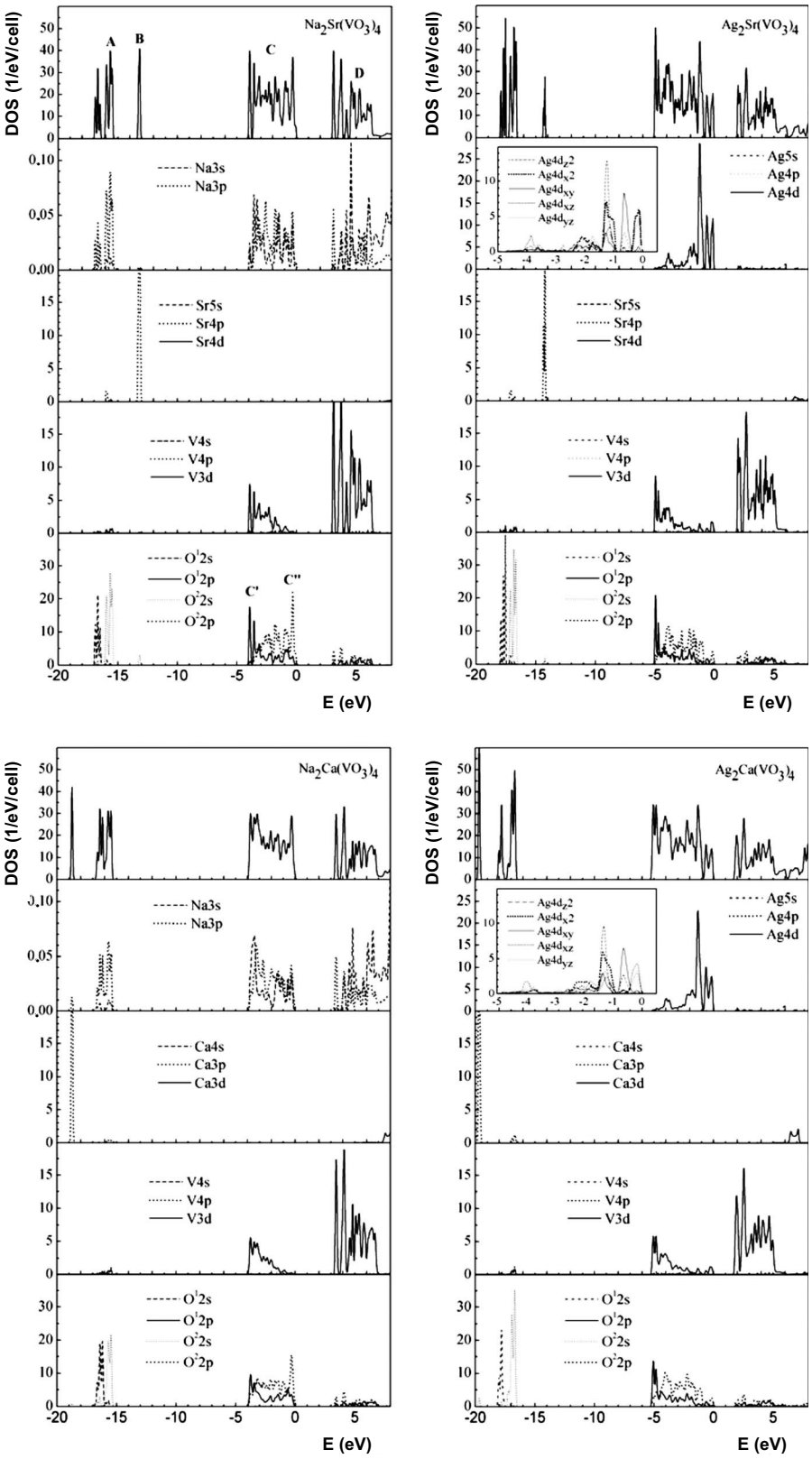

FIG. 8. Total and site-projected, *l*-decomposed DOS for cyclotetravanadates $Ag_2Ca(VO_3)_4$, $Ag_2Sr(VO_3)_4$, $Na_2Ca(VO_3)_4$, and $Na_2Sr(VO_3)_4$.

coupling parameters (C_Q=quadrupole coupling constant and η_Q=parameter of asymmetry of EFG) defined as $C_Q = (eQV_{zz})/h$ and $\eta_Q = (V_{yy} - V_{xx})/V_{zz}$, where Q is a nuclear quadrupole moment [for ^{51}V nuclei=−0.048 barn (Ref. 36)] and V_{ii} are the principal elements of the EFG tensor ($|V_{zz}| \geq |V_{xx}| \geq |V_{yy}|$) presented in Table VIII. As can be seen, the experimentally derived and calculated values of the quadrupole coupling constants C_Q reasonably agree. The discrepancy between experiment and theory is larger for the asymmetry parameters η_Q, but the main tendency within the series of cyclotetravanadates (see Table VIII) is well reproduced. Thus, the values for η_Q decrease when replacing Ca with Sr

TABLE VII. Valence band widths (in eV) for the $A_2M(VO_3)_4$ cyclotetravanadates, where A=Na, Ag and M=Sr, Ca, as obtained by FLAPW-GGA calculations.

Electronic band type	$Na_2Sr(VO_3)_4$	$Ag_2Sr(VO_3)_4$
Valence band (O $2s-E_F$)	17.10	18.05
O $2s$	1.81	1.60
Gap (O $2s$–Sr $4p$)	2.05	2.10
Sr $4p$	0.45	0.30
Gap (Sr $4p$–O $2p$+V, Ag d)	8.75	9.00
O $2p$+V $3d$	4.04	5.05
BG	2.92	2.10
Electronic band type	$Na_2Ca(VO_3)_4$	$Ag_2Ca(VO_3)_4$
Valence band (Ca $3p-E_F$)	18.91	19.95
Ca $3p$	0.25	0.24
Gap (O $2s$–Ca $3p$)	1.90	1.42
O $2s$	1.52	1.75
Gap (O $2s$–O $2p$+V, Ag d)	11.20	11.34
O $2p$+V, Ag d	4.04	5.20
BG	3.02	1.85

due to an increase in the bond lengths A-O(1,2) and M-O(2) as well as the cell volume. On the other hand, the EFG tensor for Na- and Ag-containing vanadates change in opposite directions when replacing Ca with Sr. In the Na vanadates, this tensor decreased, whereas in the Ag vanadates, it increased. This fact cannot be explained by steric effects. It is connected to the peculiarities of the redistribution of the electronic density in the two groups of vanadates. The enhancement of electric-field gradient for the ^{51}V nuclei in Ag-containing vanadates allows one to assume the presence of additional Ag-O-V interactions (in comparison to Na-containing analogs), which was also observed in the IR and Raman spectra discussed above. Note that, according to our calculations, the EFG is directed to the centers of the tetracycles, as depicted in Fig. 9. An estimate of the angles between EFG and V-O bonds shows that the EFG vector is closer to one of the two V-O(1) bonds and that increasing size of one of cations is accompanied by "alignment" of the angles between EFG and V-O(1) bonds (see Table IX).

Finally, the formation of tetracycles in $A_2M(VO_3)_4$ by $[VO_4]$ tetrahedra leads to C_Q values in the cyclotetravanadates that are one and one-half to two times larger as those for other well-known alkali metal metavanadates[37,38] wherein the vanadium nuclei are placed at slightly distorted tetrahedral sites.

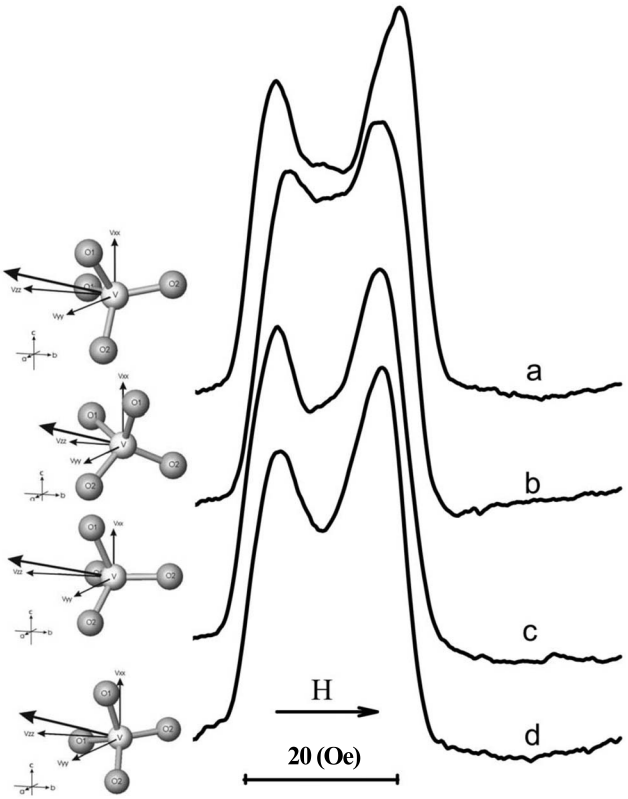

FIG. 9. The first derivatives of V^{51} NMR signals for (a) $Na_2Ca(VO_3)_4$, (b) $Na_2Sr(VO_3)_4$, (c) $Ag_2Ca(VO_3)_4$, and (d) $Ag_2Sr(VO_3)_4$. Left: the EFG vectors and their components (V_{ii}) are depicted.

IV. CONCLUSIONS

A series of cyclotetravanadates $A_2M(VO_3)_4$, where A=Na, Ag and M=Ca, Sr, has been synthesized, and an extensive investigation of their physical properties (structural, vibrational, luminescence, and electronic) has been performed by means of x-ray powder diffraction, neutron diffraction, electron diffraction, IR, Raman, NMR, and x-ray photoelec-

TABLE VIII. Quadrupole coupling constants (C_Q), parameters of asymmetry of EFG (η_Q), and the principal elements of the EFG tensor (V_{ii}) for $A_2M(VO_3)_4$ cyclotetravanadates as obtained by the NMR measurements and FLAPW-GGA calculations.

	C_Q (MHz)		η_Q		V_{ii} (10^{-21} V/cm^2)		
Compound	Expt.	Calc.	Expt.	Calc.	V_{zz}	V_{xx}	V_{yy}
$Na_2Ca(VO_3)_4$	6.4±0.5	5.88	0.21±0.03	0.407	−5.097	1.511	3.586
$Na_2Sr(VO_3)_4$	6.2±0.5	5.74	0.20±0.03	0.332	−4.972	1.661	3.311
$Ag_2Ca(VO_3)_4$	5.6±0.5	6.02	0.23±0.03	0.467	−5.176	1.380	3.796
$Ag_2Sr(VO_3)_4$	5.7±0.5	6.14	0.20±0.03	0.323	−5.287	1.788	3.499

TABLE IX. The angles (deg) between the EFG vector and V-O(1,2) bonds in the $A_2M(VO_3)_4$ cyclotetravanadates as obtained from the ^{51}V NMR data.

Compound	Angles between the EFG vector and V-O(1,2) bonds	
	V-O(1)	V-O(2)
$Na_2Ca(VO_3)_4$	45.48	84.76
	81.27	154.29
$Na_2Sr(VO_3)_4$	69.76	60.72
	80.03	170.68
$Ag_2Ca(VO_3)_4$	51.95	66.94
	93.46	154.96
$Ag_2Sr(VO_3)_4$	55.63	88.55
	66.79	156.96

tron spectroscopies, and FLAPW-GGA band structure calculations. The luminescence spectra have been obtained under pulse cathode rays and partly photoexcitation and x-ray excitation.

The structures of the $A_2M(VO_3)_4$ compounds were found to be tetragonal with the space group $P4/nbm$. The main structural feature of $A_2M(VO_3)_4$ is tetracyclic $[V_4O_{12}]$ units. The IR and Raman spectra are very sensitive to the nature of the cations because of the formation of covalent bonds (Ag-O) and the effect of the cation on the conformation of V_4O_{12} ring.

XPS and NMR techniques and the first-principles FLAPW-GGA approach have been used to investigate the electronic properties of the $A_2M(VO_3)_4$ vanadates. The oxidation states of the metal atoms are V^{5+}, Ag^+, Na^+, Ca^{2+}, and Sr^{2+}. The chemical bonding in the examined vanadates is of mixed ionic-covalent type. There are predominantly ionic interactions between alkali, alkaline-earth metals, and oxygen, while there are mixed ionic-covalent V-O and Ag-O bonds in tetracyclic units $[V_4O_{12}]$ and octahedra $[AgO_6]$, respectively. Note that there are two nonequivalent oxygen atoms O(1) and O(2), which give two groups of V-O bonds: short [V-O(2)] and long [V-O(1)] bonds.

All $A_2M(VO_3)_4$ compounds are semiconductors; the corrected band gap values from FLAPW-GGA calculations are between 4.8 [for $Na_2Ca(VO_3)_4$] and 3.0 eV [for $Ag_2Ca(VO_3)_4$], in reasonable agreement with XPS measurements. The valence spectra of the $A_2M(VO_3)_4$ compounds are similar; the top of the VB is primarily derived from hybridized O $2p-V$ $3d$ states. In $Ag_2Ca(VO_3)_4$ and $Ag_2Sr(VO_3)_4$, Ag $4d$ states are admixed into this region. When replacing Sr with isovalent Ca, the width of the near-Fermi hybridized band and the value of BG insignificantly changed (no more than 0.25 eV). On the contrary, the replacement of alkali metal (Na) with Ag leads to a more dramatic change in the $A_2M(VO_3)_4$ spectra: a significant enhancement of the hybrid bandwidth (about 1 eV) takes place accompanied by a narrowing of the BG due to the admixture of the occupied Ag $4d$ bands into near-Fermi region.

The ^{51}V quadrupole coupling parameters have been obtained, and the tendency of their changes in a series of cyclotetravanadates explained. Finally, among the most interesting characteristics of these materials are their luminescence properties. According to our data, the intrinsic luminescence spectra for Na- and Ag-containing $A_2M(VO_3)_4$ cyclotetravanadates correspond to luminescence centers connected to the decay (relaxation) of self-trapped excitons on some lattice defects, including distortion of vanadate VO_4 units, electronic F, and hole O^- centers. The analysis of luminescence spectra of these materials shows that they represent a superposition of the bands in green, orange, red, and deep red regions of the spectrum. Additionally, these materials demonstrate a pronounced selective sensitivity of separated bands (for example, the 698 nm band) to type of excitation (photon or corpuscular radiation) and to photon excitation energy, in comparison with other known vanadates.[1–7] This effect may be important for the development of detectors with a selective sensitivity for photon and corpuscular radiation. The $Na_2M(VO_3)_4$ compounds with their white-green luminescence have potential for development of LEDs. The $Ag_2M(VO_3)_4$ compounds are not suitable for development of LEDs, due to their weak light output, but they could be interesting for color correction of light emission from sources including lamp and LED sources.

ACKNOWLEDGMENTS

This work was supported by the Russian Foundation for Scientific Schools under Grant No. SS 5138.2006.3, the Russian Foundation for Basic Research under Grants No. 05-03-32307 and No. 07-03-00143, and ICDD Grant-in-Aid under Grant No. 93-09 (2001). The authors are grateful to Olga V. Koryakova, Emma G. Vovkotrub, and Viktor N. Strekalovskii for the technical assistance.

*gunnar@struc.su.se

[1] J. R. O'Connor, Appl. Phys. Lett. **9**, 407 (1966).
[2] G. Blasse and A. Bril, J. Chem. Phys. **50**, 2974 (1969).
[3] A. A. Fotiev, B. V. Shulgin, A. S. Moskvin, and F. F. Gavrilov, *Vanadate Crystallophosphors* (Nauka, Moscow, 1976).
[4] A. A. Fotiev, B. V. Slobodin, and M. Ya. Khodos, *Vanadates, Composition, Synthesis, Structure, Properties* (Nauka, Moscow, 1988).
[5] B. V. Slobodin and L. L. Surat, Russ. J. Inorg. Chem. **47**, 1349 (2002).
[6] V. G. Zubkov, A. P. Tyutyunnik, I. F. Berger, L. L. Surat, and B. V. Slobodin, Russ. J. Inorg. Chem. **48**, 1915 (2003).
[7] B. V. Slobodin, L. L. Surat, V. G. Zubkov, A. P. Tyutyunnik, I. F. Berger, M. V. Kuznetsov, L. A. Perelyaeva, I. R. Shein, A. L. Ivanovskii, B. V. Shulgin, V. I. Solomonov, G. Svensson, B. Forslund, and M. J. Sayagués, Phys. Rev. B **72**, 155205 (2005).
[8] I. Tordjman, C. Martin, and A. Durif, Bull. Soc. Fr. Mineral. Cristallogr. **90**, 293 (1967).

[9] C. Cavero-Ghersi and A. Durif, J. Appl. Crystallogr. **8**, 562 (1975).
[10] M. T. Averbuch-Pouchot and A. Durif, Acta Crystallogr., Sect. C: Cryst. Struct. Commun. **39**, 811 (1983).
[11] M. T. Averbuch-Pouchot, Eur. J. Solid State Inorg. Chem. **33**, 15 (1996).
[12] M. Graia, A. Driss, and T. Jouini, Z. Kristallogr. - New Cryst. Struct. **214**, 1 (1999).
[13] H. Yamane, R. Tanimura, T. Yamada, J. Takahashi, T. Kajiwara, and M. Shimada, J. Solid State Chem. **179**, 289 (2006).
[14] T. I. Krasnenko, O. A. Zabara, A. A. Fotiev, and A. N. Egorov, Inorg. Mater. **27**, 1100 (1991).
[15] B. V. Slobodin and N. V. Kiseleva, Russ. J. Inorg. Chem. **34**, 2976 (1989).
[16] A. C. Larson and R. B. Von Dreele, "General Structure Analysis System (GSAS)," Los Alamos National Laboratory Report No. LAUR 86-748 (2000).
[17] A. P. Tyutyunnik, V. G. Zubkov, L. L. Surat, and B. V. Slobodin, Powder Diffr. **20**, 189 (2005).
[18] R. N. Pletnev, V. A. Gubanov, and A. A. Fotiev, *NMR in Vanadium Oxides* (Nauka, Moscow, 1979).
[19] P. Blaha, K. Schwarz, G. K. H. Madsen, D. Kvasnicka, and J. Luitz, in *WIEN2K, An Augmented Plane Wave Plus Local Orbitals Program for Calculating Crystal Properties*, edited by K. Schwarz (Techische Universität Wien, Austria, 2001).
[20] J. P. Perdew, K. Burke, and M. Ernzerhof, Phys. Rev. Lett. **77**, 3865 (1996).
[21] P. E. Blöchl, O. Jepsen, and O. K. Andersen, Phys. Rev. B **49**, 16223 (1994).
[22] R. D. Shannon, Acta Crystallogr., Sect. A: Cryst. Phys., Diffr., Theor. Gen. Crystallogr. **32**, 751 (1976).
[23] A. F. Wells, *Structural Inorganic Chemistry* (Oxford University Press, Oxford, England, 1986).
[24] J. Mink and L. Mink, *Computer Program System for Vibrational Analysis of Polyatomic Molecules* (Laney-Fujitsu Fortran Win 32, Stockholm, 2004).
[25] S. Polosan, M. Bettinelli, and T. Tsuboi, Conference Program and Book of Abstracts of Tenth Europhysical Conference on Defects in Insulating Materials (University of Milano, Bicocca, 2006), p. 62.
[26] C. Shi, Y. Wei, X. Yang, D. Zhou, C. Guo, J. Liao, and H. Tang, Chem. Phys. Lett. **328**, 1 (2000).
[27] D. Millers, H. M. Yochum, V. Pankratov, P. Potera, and L. Grigorjeva, Phys. Status Solidi C **4**, 1155 (2007).
[28] S. Polosan, M. Bettinelli, and T. Tsuboi, Phys. Status Solidi C **4**, 1352 (2007).
[29] L. J. Sham and M. Schluter, Phys. Rev. Lett. **51**, 1888 (1983).
[30] J. Robertson, J. Vac. Sci. Technol. B **18**, 1785 (2000).
[31] P. W. Peacock and J. Robertson, J. Appl. Phys. **92**, 4712 (2002).
[32] J. Robertson, K. Xiong, and S. J. Clark, Thin Solid Films **496**, 1 (2006).
[33] S. Tang, R. Wallace, A. Seabaugh, and D. King-Smith, Appl. Surf. Sci. **135**, 137 (1998).
[34] C. B. Samantaray, H. Sim, and H. Hwang, Microelectron. J. **35**, 655 (2004).
[35] A. Abragam, *The Principles of Nuclear Magnetism* (Clarendon, Oxford, 1961).
[36] M. R. Hansen, G. K. H. Madsen, H. J. Jakobsen, and J. Skibster, J. Phys. Chem. B **110**, 5975 (2006).
[37] J. Skibsted, N. Chr. Nielsen, H. Bildsere, and H. J. Jakobsen, J. Am. Chem. Soc. **115**, 7351 (1993).
[38] O. B. Lapina, A. A. Shubin, D. F. Khabibulin, V. V. Terskikh, P. R. Bodart, and J.-P. Amoureux, Catal. Today **78**, 91 (2003).